Molecular rotor-rotor heat diffusion at the origin of the enhanced thermal conductivity of hybrid perovskites at high temperatures

Ashutosh Giri,[*,†] Sandip Thakur,[†] and Alessandro Mattoni[*,‡]

†*Department of Mechanical, Industrial and Systems Engineering, University of Rhode Island, Kingston, RI 02881, USA*

‡*Istituto Officina dei Materiali (CNR- IOM) Cagliari, SLACS, Cittadella Universitaria, I-09042 Monserrato, CA, Italy*

E-mail: ashgiri@uri.edu; mattoni@iom.cnr.it

Abstract

We demonstrate a new regime of heat conduction in hybrid metal halide perovskites where the thermal conductivity increases with temperature due to the rotational and librational motion of the organic cations. Our molecular dynamics simulations on $MAPbI_3$ show that as the temperature is increased across the orthorombic-tetragonal-cubic phase transitions, the contributions to the total thermal conductivity from the organic cations monotonically increases to $\sim$60%, whereas the contributions from the inorganic framework decrease with a similar temperature dependence that is often associated with anharmonic phonon scattering processes of crystalline solids. The increase in the organic constituent contributions to the total thermal conductivity as temperature is increased leads to a temperature-independent thermal conductivity at high temperatures. By comparing $MAPbI_3$ results with the corresponding inorganic $CsPbI_3$ lead halide (by using a new specifically designed MYP parametrization) we unambiguously ascribe the unique temperature trend of the hybrid perovskite to the collective rotational motion

of the organic molecules leading to additional channels of heat flow at higher temperatures in these materials. Our findings are relevant for the thermal stability of hybrid perovskites to optimize heat dissipation and working conditions in optoelectronic, thermoelectric, and phononic devices based on hybrid perovskites.

Keywords: Metal halide perovskites, temperature-dependent thermal conductivity, heat conduction, hybrid inorganic-organic materials, phase transitions

Metal halides perovskites have garnered tremendous amount of attention in recent years due to their remarkable structure-property relationships, which makes them ideal candidates for use in emerging technologies such as in electrochemical energy storage, thermoelectric applications and primarily in solar cells.[1–9] The crystalline perovskite structure of formula ABX_3 is formed by a three-dimensional BX_3 network of corner sharing octahedra with metals (e.g. Pb) at the centers and halide anions (I,Br) at the corners. Positively charged cations occupy the A sites of the perovskite lattice. Cations of large radii are necessary to make the crystal structure stable. In the case of organic cations (e.g. methyalmmonium CH_3NH_3, MA) a hybrid organic-inorganic perovskite is obtained. This is the case of the celebrated $MAPbI_3$ crystal, which has emerged as one of the most efficient photovoltaic solution-processable semiconductor.[10,11] Central to these applications, however, is the comprehensive understanding of their thermal transport properties. In this regard, recent studies have shown that their ultralow thermal conductivity mainly derives from the low group velocities of acoustic phonons that in turn derives from the soft nature of the lead halides crystals in addition to strong anharmonic phonon-phonon scattering mechanisms.[12–15] Considering the reduced thermal stability[16] and the promising thermoelectric properties of metal halides[17], understanding and controlling the heat flux is crucially important to improve material stability, to optimize working temperature and thermodynamics conditions of devices, and to design nanosystems for heat management.

In general, for most non-metallic solids and for the lattice contribution in metals, heat conduction theories (dating back to the work by Peirels in 1929)[18] are generally rooted in the phonon gas models.[19–21] In these models, heat is primarily carried by propagating phonon wavepackets and re-

sistive processes such as anharmonic phonon-phonon scattering mechanisms generally dictate the temperature dependent thermal conductivity (for defect-free crystalline solids at intermediate and high temperatures).[22,23] However, for disordered solids and complex crystals, theories reliant on the phonon gas models are not able to fully capture the heat conduction mechanisms due to the fact that a substantial contribution from non-propagating vibrations (with mean-free-paths on the order of the average atomic spacings) can dictate the temperature dependent thermal conductivities.[24–26] In such cases where the Peierls's phonon picture breaks down, Allen and Feldman's harmonic theory for glasses where the coupling of vibrational modes arising from the off-diagonal elements of the velocity operator has been successful in describing glass-like heat conduction.[25,27–29]

The mechanism of thermal transport in metal halide perovskites is at the intersection of these two regimes, i.e. crystal-like and glass-like.[26,27] The inherent disorder of the soft metal halide crystals (forming the BX_3 network) along with the hybridization of vibrational modes between the inorganic framework and the host species (occupying the A sites) renders the conventional phonon picture of thermal transport insufficient. As such, a combination of mixed phononic and non-phononic features associated to a peculiar glass-crystal duality has been proposed for these types of materials.[26] The low frequency modes, that are mainly due the inorganic lattice,[30] retain features of acoustic waves but exhibit short lifetimes of a few tens of picoseconds. Anharmonic effects (two orders of magnitude higher than in silicon) occur within such wave-like modes as well as between modes of the octahedral framework and modes localized at the A cations (e.g. anharmonic rattling dynamics of Cs).[31] Recently a transport equation has been derived for a unified theory of thermal conductivity in solids[27] consisting of two contributions that are appropriately named 'populations' (i.e. particle-like phonon wavepackets of Peierls' semiclassical picture) and 'coherences' (wave-like tunneling and loss of coherence between different vibrational eigenstates). In anharmonic crystals or harmonic glasses the two terms reduce to the Peierls and Allen-Feldman limits, respectively. As for the temperature dependence, the phononic-term decreases as T^{-1} according to phonon-phonon Umklapp scattering, while the 'coherences' term, similar to the Allen-Feldman theory, increases with temperature. The overall behavior depends on the relative weight of the two

terms. For the inorganic perovskite $CsPbBr_3$ at room temperature, it was found that the 'populations' term is minor (just 30% of the total conductivity) while the 'coherences' term provides a large 70% contribution.[27] Despite the major non-phononic contribution, the thermal conductivity of the inorganic $CsPbBr_3$ decreases with temperature, albeit with a reduced temperature dependence than the T^{-1} that is usually attributed to Umklapp scattering processes in perfect crystals.

To our knowledge there are no metal halide crystals for which the thermal conductivity at high-temperature does not decrease with temperature. The crystal-glass duality is expected, *a fortiori*, for hybrid metal halides. The presence of molecular cations induce localized vibrational states and disorder due to molecular configurations and thermally activated reorientations of the molecules.[32] Moreover, for such guest-host systems, the dynamic motion of the guest atoms are generally associated with reduction in thermal conductivity through hybridized coupling of vibrations between the guest and the host lattice.[31,33–35] Even for hybrid metal halide perovskites, many studies have hypothesized that the low thermal conductivities in these materials derive from the dynamics of the organic molecules and their coupling with the inorganic lattice.[34–38] This is in qualitative agreement with the blurring of the optical modes due to MA motion at finite temperature[26] but it is in quantitative contrast to the reduction of thermal conductivity found for systems in which the MA rotations were selectively frozen.[39,40] In addition, the room temperature thermal conductivity of inorganic lead halides (e.g. $CsPbI_3$) is comparable to that of the hybrid counterparts (0.4-0.5 W m^{-1} K^{-1}).[12,27,31] Accordingly, the effect of molecules in hybrid perovskites is more complex than just a source of scattering and lowering of the thermal conductivity.

Here, the thermal conductivity of $MAPbI_3$ is studied by molecular dynamics (MD) simulations across a wide range of temperatures and compared to fully inorganic $CsPbI_3$ perovskites for which we report here the new force-field parameters. We demonstrate a mechanism of heat transfer where the rotational motion of the organic cations inside the inorganic framework can lead to a non-phononic trend (that is the typical $1/T$ behavior due to anharmonic scattering) in the thermal conductivity. In the low-temperature orthorhombic crystal, the contributions from the inorganic framework dominate the thermal conductivity. However, as the temperature is increased across the

tetragonal and cubic phases, the contributions from the inorganic framework decreases following the anharmonic phonon scattering expected for crystalline solids while the contributions from the organic cations monotonically increases by up to $\sim$50%, giving rise to an overall temperature independent thermal conductivity at higher temperature. This anomalous and nonmonotonic temperature dependence is a macroscopic manifestation of a glass-like behavior of the crystal associated with the dynamics of molecules that contribute to heat diffusion through rotor-rotor interactions. Accordingly, at high temperatures the molecules, instead of suppressing transport, can contribute substantially to the overall thermal conductivity. This behavior is unambiguously attributed to molecular rotations by comparing the case of hybrid perovskites to their inorganic counterpart as well as by fictitiously rescaling masses or inhibiting rotations. Besides the fundamental relevance, the present results show that the rotational molecular dynamics can be tuned so as to enhance rather than suppress thermal conductivity.

Experimental measurements of thermal conductivity of hybrid perovskites above room temperature are challenging because of the aforementioned material thermodynamic instability. Real samples degrade at $\sim$150 °C through the formation of inorganic PbI_2 that further decomposes at 550 and 600 °C.[16] Encapsulated systems have shown to be stable at higher temperatures indicating that the intrinsic thermal stability of the material is higher and encapsulation provides a route for improving it.[41] Here, we apply atomistic simulations that make it possible to study intrinsic properties of perfect crystals and explore thermal conductivity over a wide range of temperatures excluding the effects of surfaces, interfaces and defects that dominate the onset of degradation in real samples. The knowledge of temperature-dependence of thermal conductivity at high temperatures (i.e. the function $\kappa(T)$) is relevant for solar cells under direct or concentrated light and for device processing requiring various heating steps that can help optimize the heat dissipation and the film's stability.

For our atomistic simulations, we implement the interatomic potential developed by Mattoni *et al.*,[32] which has been used previously to study the thermal properties of $MAPbI_3$.[14,37,39] The model takes into account dispersive and long-range electrostatic interactions[42] and it has demonstrated the

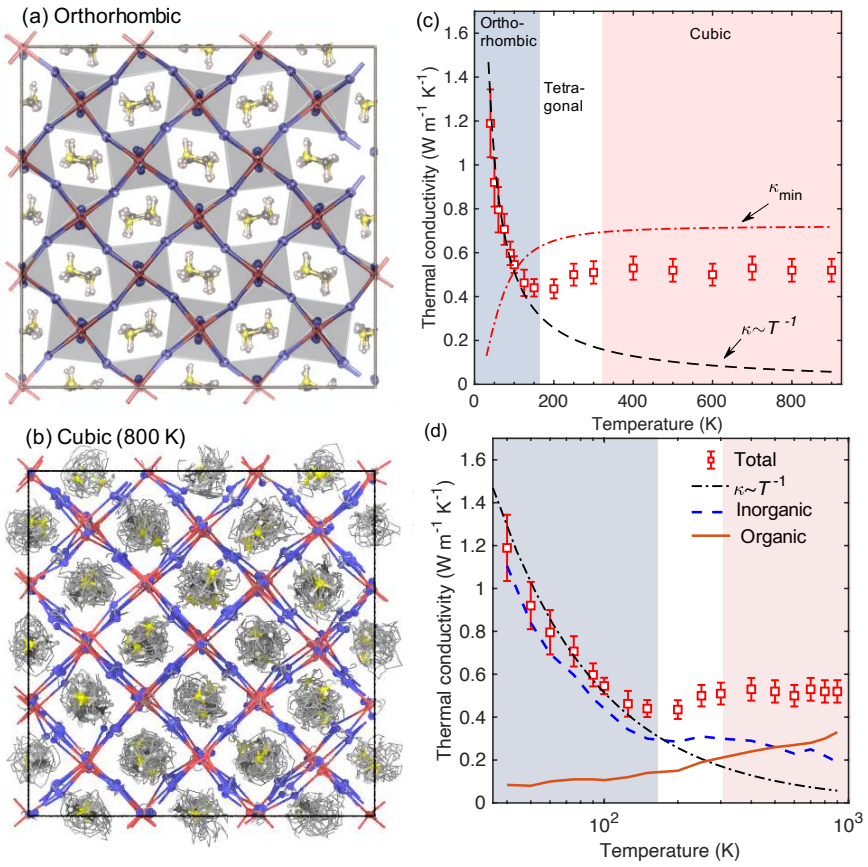

Figure 1: (a) Snapshot of our $MAPbI_3$ computational domain representing the orthorhombic phase at 50 K. (b) Snapshots at 800 K temperature showing trajectory lines calculated for a total of 0.5 ps at 50 fs intervals for $MAPbI_3$. The trajectory lines demonstrate that the cations perform free rotational and librational motions in the $MAPbI_3$ structure. (c) Equilibrium molecular dynamics-predicted thermal conductivity of $MAPbI_3$ as a function of temperature. For comparison, the dashed-dotted line shows predictions from the minimum thermal conductivity model. In the orthorhombic phase, thermal conductivity follows the $\kappa \sim T^{-1}$ trend characteristic of phonon scattering due to anharmonic effects. As temperature is increased across the tetragonal-cubic phases, thermal conductivity deviates considerably from the T^{-1} trend. (d) Contributions from the inorganic (dashed-line) and organic (solid line) constituents as a function of temperature.

ability to reproduce a wide range of material properties including, for example, structures and vibrations[30], elastic properties, ionic polarization[43,44] and mobility.[45] For the purposes of the present study, we remark that the model describes correctly not only the structure-temperature relationship (lattice parameters, thermal expansion and phases transitions) but it also describes accurately the hybrid organic-inorganic interactions and the reorientational dynamics of the MA molecules. At low temperatures the direction of organic MA cations (and associated dipoles) are constrained by the network of PbI_6 octahedra (with $a^-b^-c^+$ Glazer tilting) in the Pnma orthorhombic crystal structure as shown in Fig. 1a. Above the orthorhombic-to-tetragonal transition (correctly reproduced by the model at $\sim$160 K), for the tetragonal phase with $a^0a^0c^-$, the molecular trajectories exhibit a change from small fluctuations about high symmetry directions to a fast dynamics in which the dipoles can reorient quasi-randomly on the spherical surface as quantitatively shown in the schematic in Fig. 1b by the trajectory lines of the MA cations. The transition in the MA dynamics is correlated to the inorganic lattice evolution. The Pb-I bond lengths along with the total volume of the computational domain increase with temperature resulting in a larger nanocage volume for the dynamical motion of the organic cations (as shown in Fig. S3 of the SI). Therefore, based on the above discussions, we consider the choice of the potential appropriate in describing the changes in the thermal properties with temperature that we discuss next.

To gain insights into the temperature dependent thermal transport properties of $MAPbI_3$, we calculate the thermal conductivities in a wide temperature range (40 K to 850 K) from equilibrium molecular dynamics (EMD) simulations; see SI for further details of the simulations including the calculation of the heat flux autocorrelation function and the time integral for the equilibrium calculations. Figure 1c shows the temperature dependent thermal conductivity of $MAPbI_3$ predicted from our EMD calculations. In the orthorhombic phase, the temperature dependent thermal conductivity of $MAPbI_3$ shows a power-law decay $1/T^u$ (see Fig. 1c) with the exponent $u \sim 1$ consistent with anharmonic Umklapp scattering in defect free, crystalline solids.[22,23] However, as the temperature is increased across the tetragonal and cubic phases, thermal conductivity shows a temperature independent trend and clearly deviates from the temperature trend that is generally as-

sociated with anharmonic phonon scattering processes. Accordingly, present MD analysis shows strong deviations from the phononic picture and a transition to a non-phononic (i.e. glass-like regime).

In Fig. 1c, we also plot the predictions from a minimum limit to thermal conductivity model that is often applied to pure amorphous solids where non-propagating vibrations are the dominant heat conduction channels.[24] The main assumptions in this model are that the "mean-free-paths" of vibrations in the solid are limited to the spacing between adjacent atoms and the lifetimes of these heat-carrying oscillations are one half the period of vibration (see SI for details).[46] In the tetragonal and cubic phases, our EMD-predicted thermal conductivities are below this minimum limit. This suggests that heat conduction in $MAPbI_3$ can not solely be explained by energy propagation mediated through thermal interactions on the length scale of the vibrational wavelength. As anticipated, this result is in contrast to the attribution of the low thermal conductivity solely due to strong acoustic-optical phonon scattering resulting from the severe overlap of corresponding dispersion branches.

We separate the contributions from the inorganic and organic constituents for the temperature range studied as shown in Fig. 1d. The inorganic constituents dominate heat conduction at lower temperatures in the orthorhombic phase (as represented by the dashed-line in Fig. 1d). However, as temperature increases, the contribution from the inorganic framework decreases in a similar qualitative trend as compared to $\sim T^{-1}$. This is in contrast to the overall increasing behavior of the total thermal conductivity of $MAPbI_3$ at higher temperatures. The temperature dependent contributions from the organic constituent is drastically different with minimal contribution in the orthorhombic phase, which increases remarkably as temperature is increased. The inorganic and organic components contribute equally at room temperature while at higher temperatures, the organic constituents dominate heat flow with $\sim$65% contribution to the total thermal conductivity at $\sim$850 K. Note, the transition from inorganic framework dominated heat conduction to that dominated by the organic cations occurs around the orthorhombic to tetragonal phase transition at which molecular reorientations are activated and this highlights the role of the guest-host interactions in the nanocages (see

Fig. S5) in dictating heat transfer mechanisms in these materials.

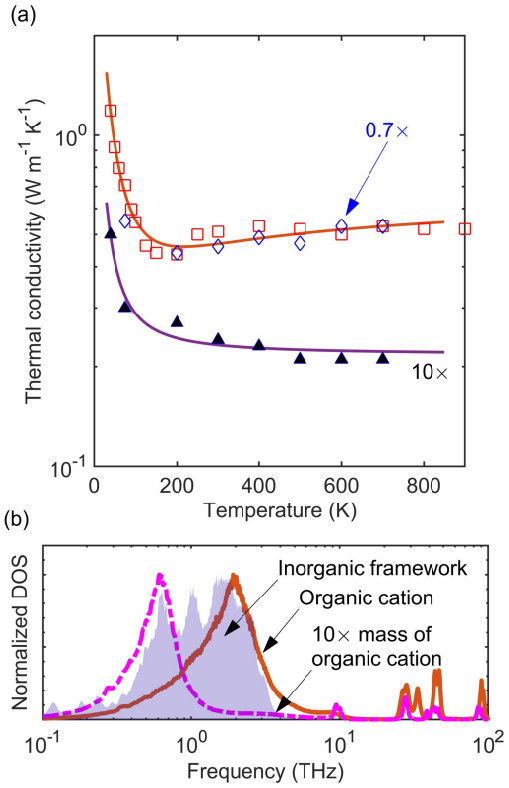

Figure 2: (a) Thermal conductivity as a function of temperature for our $MAPbI_3$ structures with fictitiously different masses of the organic cations. We fit the temperature-dependent thermal conductivity for the different structures with the model: $\kappa(T) = \left(\frac{T_1}{T}\right)^u + e^{\frac{-E_b}{k_B T}} \left(\frac{T}{T_2}\right)^c$ (see text). (b) Vibrational density of states for the organic cations with 10× the mass of carbon and nitrogen atoms compared to that of the realistic structure. The low frequency vibrations of the organic cations shift to the lower frequencies with increasing mass.

To better understand the role of dynamic motion of organic cations, we run additional simulations on $MAPbI_3$ structures with fictitious masses for the carbon and nitrogen atoms with masses perturbed by 0.7× and 10× compared to their realistic masses. Figure 2a shows the temperature dependent thermal conductivities of different structures with the mass perturbed organic cations. First of all, we observe that by increasing the mass of the cations the $\kappa(T)$ curve is lowered and the thermal conductivity decreases at each temperature. This is consistent with the giant MA isotope effects measured recently.[47] The reduction of κ with mass is expected in disordered solids (e.g. gases) because atom velocities and scattering frequency scales as $\sqrt{\frac{T}{m}}$ (at equilibrium

$mv^2 \sim k_B T$). Conversely, the $0.7\times$ mass perturbed case shows similar thermal conductivities to the mass unperturbed case. This is so because the rotational and librational dynamics of the MA cations with $0.7\times$ masses are not significantly changed as compared to our unperturbed structure; further analysis of the rotational motion by comparing the mean square displacements of the mass perturbed cases show that the dynamics of the MA cations do not change when their masses are decreased (see Fig. S13). However, increasing the mass to $10\times$ leads to severely hindered rotational motion of the organic cations, which concomitantly results in a significantly different $\kappa(T)$ for the $10\times$ case as shown in Fig. 2a. This again demonstrates that the rotational motion of the cations are key to the unique temperature behavior of thermal conductivity for $MAPbI_3$. We note here that a comparison to hybrid perovskites with different cation species such as with bulkier organic constituents would elucidate the role of different degrees of freedom on the thermal transport properties. However, these calculations need extensive validation of the interatomic potentials describing the interactions of the organic species with the inorganic framework and are therefore outside the scope of the current work but deserve further investigation in future works.

This peculiar T dependence can be modeled as the sum of two terms: a decreasing term ($\kappa \sim T^{-u}$) and an Arrhenius-like one $e^{-E_b/k_B T}\left(\frac{T}{T_C}\right)^c$, where E_b is the energy barrier controlling the temperature dependence. Results of fitting is reported in Fig. 2a (as the solid red line) and the values for u and E_b are 1 and ~ 30 meV, respectively. The value of E_b is close to the activation energy for molecular rotations and is independent of mass for the lower mass case. Note, the rotational motion of the cations in the $MAPbI_3$ structure and for the case of $0.7\times$ mass are very similar as determined by the mean square displacement calculations (see Fig. S13). This further supports our observation that the rotational and librational degrees of freedom are related to the increase of thermal conductivity with temperature. The independence of E_b on the mass (as observed for the $0.7\times$ and $1\times$ cases) is consistent with the fact that the masses affect the dynamics of the molecule but not the interatomic forces and energy barrier for rotation, which only depend on the atomic partial charges and potential parameters.

Our interpretation of the results is that the increase of $\kappa(T)$ is related to the contribution to

thermal conductivity coming from rotations of the organic cations. According to our previous analysis,[32] the rate of rotation follows an Arrhenius behavior $\nu e^{-E_b/kT}$; E_b is constant but the frequency ν (i.e. the rotational frequency of cations) described as a rigid rotor of inertia moment I decreases with increasing mass ($\nu \sim \sqrt{\frac{k_B T}{I}} \sim m^{-\frac{1}{2}}$). Accordingly, with increasing mass of the cations the rate of rotation becomes progressively slower and the contribution from these modes to the overall $\kappa(T)$ decreases.

In order to bolster this hypothesis we also consider the effects of other factors such as the overlap of organic/inorganic vibrational bands. As anticipated, with a heavier cation mass, the vibrations associated with the rotation, translation, spinning and twisting of the molecules shift to lower frequencies and the vibrations in the higher frequency range are diminished as compared to the case for cations with the realistic masses (see Fig. 2b for comparison of DOS for structures with 10$\times$ masses and that for structures with the realistic masses of the carbon and nitrogen atoms). Furthermore, by considering fictitiously heavier masses for the PbI cages, we confirm that the overlap between the DOS of the inorganic and organic cations does not influence the increasing trend in thermal conductivity at higher temperatures (see Fig. S10). This suggests that the range of vibrational spectrum of the guest molecules (more-so than the vibrational spectrum of the PbI framework and its' overlap with the DOS of the organic cations) dictates the temperature-dependent thermal conductivity at high temperatures.

Next, to gain further support to argue that the anomalous behaviour of $\kappa(T)$ is mainly ascribed to the rotational and librational dynamics and not to other degrees of freedom of the MA cations, we perform additional simulations on structures where we constrain the rotational motion of the molecules. For this, we decrease the amount of free space for the motion of MA cations by shrinking the nanocage volume by applying pressure as schematically shown in Fig. 3a; the trajectory lines for MA cations are calculated for a total of 0.5 ps at 50 fs intervals (at 800 K). The smaller volume of the inorganic cages restricts the rotational motion as represented by the fairly restricted trajectory lines as compared to that for the $MAPbI_3$ structure with the regular octahedral cage volume (see Fig. 1b showing cations performing free rotational and librational motions).

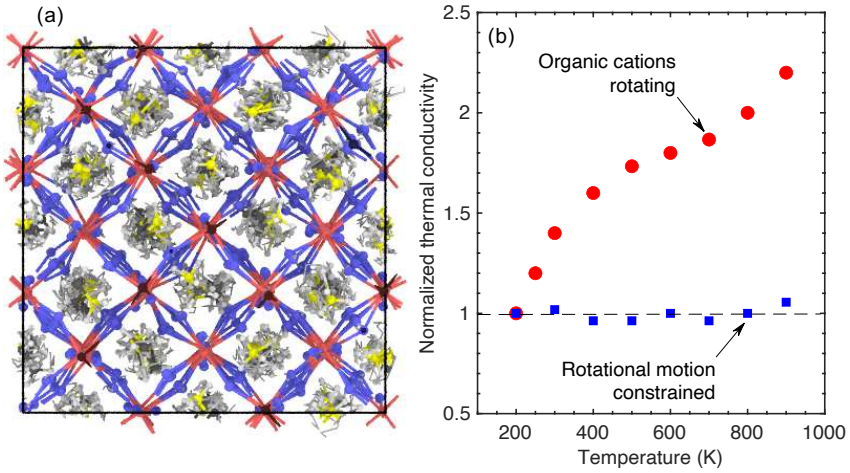

Figure 3: (a) Snapshot at 800 K temperature showing trajectory lines calculated for a total of 0.5 ps at 50 fs intervals for $MAPbI_3$ where the octahedral cages are reduced in size to constrain the rotational motion of methylammounium cations. The smaller inorganic cages in the constrained case restrict the rotational motion as shown by the calculated trajectory lines. (b) Normalized thermal conductivity contributions from the organic cations for the $MAPbI_3$ unconstrained case (where the organic cations rotate freely; red circles) and for the constrained case (where the organic cations do not perform free rotations; blue squares). Note, the thermal conductivities have been normalized by their respective thermal conductivity values for the organic cations calculated at 200 K. In contrast to the unconstrained $MAPbI_3$, for the computational domain with smaller octahedral cages that constrain the rotational motion of the methylammonium cations, the normalized values are $\sim$1 for the entire temperature range suggesting that the thermal conductivity contribution from the organic cations does not increase with temperature.

This translates to drastically different $\kappa(T)$ trends of the organic cations between the two cases as shown in Fig. 3b where we plot the contributions from the organic cations to the temperature dependent thermal conductivities normalized with respect to their room temperature thermal conductivity contributions for comparison. The lack of temperature dependence for the constrained case suggests that drastically different (and increasing) trend in $\kappa(T)$ of the MA cations for the case of the $MAPbI_3$ structure with the regular octahedral cage volume is related to the MA cations performing rotational and librational motions.

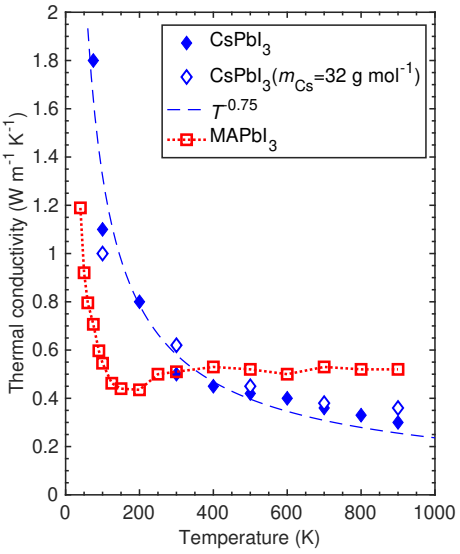

Figure 4: (a) Thermal conductivity as a function of temperature for $MAPbI_3$ compared to that of $CsPbI_3$ and for a $CsPbI_3$ with the mass of Cs atoms fictitiously reduced to match the mass of methylammonium inside the PbI_6 octahedra. Unlike the temperature dependence of $MAPbI_3$, for the $CsPbI_3$ structures, the thermal conductivity decreases (with $\sim T^{-0.75}$ trend) throughout the temperature range studied. The guest Cs atoms do not contribute substantially at higher temperatures in contrast to $MAPbI_3$.

Finally, in order to unambiguously confirm that the anomalous temperature dependence must be ascribed to molecular rotations and to the hybrid nature of the material, we run comparative simulations on the inorganic counterpart, i.e. $CsPbI_3$ with heavy cesium ions ($\sim$ 132 amu) replacing the MA molecules ($\sim$ 32 amu). To this aim, we have developed a specific force-field with identical Pb-I interactions, the details for which can be found in the SI. We note that the model

reproduces phase transitions and lattice parameter of $CsPbI_3$ with temperature. Figure 4 shows the temperature dependent thermal conductivity of $CsPbI_3$. In contrast to the temperature dependent thermal conductivity of $MAPbI_3$, we find a monotonic decrease with a $\sim T^{-0.75}$ trend for our all inorganic system. The deviation from a typical (T^{-1}) Umklapp scattering dominated temperature response can be ascribed to phonon scattering and hybridization due to guest-host interactions as has been previously demonstrated.[31,48,49] Moreover, perturbing the mass of the cesium cations (to mimic the mass of the light MA molecules in $MAPbI_3$) also does not significantly modify the temperature trend suggesting that the shift of vibrational frequencies to a higher spectral regime does not lead to an increase in thermal conductivity at higher temperatures (see Fig. S12 for the DOS of the cesium cations and the inorganic framework for the $CsPbI_3$ domain). We note that the hybrid and inorganic models have identical Pb-I interactions and similar values of point-like interactions (the Cs-Pb and Cs-I parameters are similar to the parameters of the N, C-Pb and N,C-I interactions). Therefore, different $\kappa(T)$ behavior between the all inorganic and the hybrid structures must be ascribed to the (dipolar/multipolar) structure of the MA cations and to the associated rotational dynamics in the hybrid system. The fact that $CsPbI_3$ thermal conductivity is almost independent on the Cs mass (see Figure 4) is consistent with the behavior of a crystalline material; in fact, κ scales with the speed of sound that is almost independent on the mass of the A cation (see Fig. S14 of SI). It is also interesting to note that at temperatures above $\sim$200 K, the contributions to $\kappa(T)$ from just the inorganic framework in $MAPbI_3$ deviates considerably from the ideal T^{-1} trend for pure crystalline solids (more-so than the $\kappa(T)$ trend for $CsPbI_3$) as shown in Fig. 1d. This temperature independence in $\kappa(T)$ for the contributions of the inorganic PbI framework is due to the pronounced vibrational scattering introduced from the rotational and librational degrees of freedom of the MA cations at higher temperatures as compared to the case of Cs atoms with fewer degrees of freedom. Taken together, these observations highlight the unique 'dual glass-crystal' thermal response of the hybrid $MAPbI_3$ structure at high temperatures.

We summarize our findings on the origin of the glass-like behavior and the corresponding anomalous T dependence of $\kappa(T)$: (i) the effect is due to the organic molecules; it persists while

changing the masses of the PbI atoms but it disappears when replacing the molecules by ions (as in $CsPbI_3$ perovskites) independent of their mass. (ii) the effect is linked to the rotations (and not to other internal degrees of freedom of the molecule); in fact, the trend disappears in compressed perovskites where rotations are inhibited but internal degrees of freedom are not. The role of rotations is further supported by three additional observations: (i) the temperatures at which the effect occurs correspond to those at which the rotations are thermally activated; (ii) the fitted thermal activation in $\kappa(T)$ are compatible with the activation energy for molecular rotations (~ 30 meV); (iii) the rotational contribution can be tuned by changing the molecular masses, m.

The suppressed thermal conductivity in materials with guest-host interactions in general has been attributed to coupling and hybridization of the guest-host vibrational modes leading to avoided crossings and flat bands.[33,49,50] Our results and analysis presented in this study suggest that the guest-host vibrational mode coupling not only leads to suppressed thermal conductivity, but can also lead to competing effects dictating the heat conduction in hybrid inorganic-organic perovskites where the collective rotational motion of the organic molecules can enhance thermal conductivity at higher temperatures. In other words, the dynamic motion of the organic guest molecules inside the inorganic octahedra can enhance anharmonic phonon scattering processes that lowers the thermal conductivity or it can also lead to additional heat transfer channels thus increasing the total thermal conductivity. Considering that the organic contribution to thermal conductivity of $MAPbI_3$ is dominated by electrostatic forces (see Fig. S4 of the SI) we conclude that the increasing heat transfer channel must be rooted on the dipole-dipole interactions between molecular rotors that are absent in the case of point-like cesium cations. This is consistent with the increase in the dielectric function observed in $MAPbI_3$ at the orthorhombic-to-tetragonal transition (and not in the inorganic $CsPbI_3$) and due to electric polarization by molecular reorientations.[42] This marks a new mechanism of thermal transport in crystalline solids where the collective rotational motion of guest species can facilitate heat conduction at high temperatures. The insights gained from such high-temperature-driven thermodynamic changes present an ideal platform to understand the intrinsic structure-property relationship that are otherwise not obvious at ambient temperatures. Our study

provides guidelines for future and next-generation hybrid materials by design for applications in photovoltaics and flexible energy harvesting devices that have the potential to redefine how we generate, store and use energy.

Acknowledgement

This manuscript is based upon work supported by the Office of Naval Research, Grant No. N00014-21-1-2622. A. M. acknowledges Italian Ministry MUR for funding though project PON04a2 00490 "M2M Netergit", Italian National Research Council CNR for for projects CNR-RFBR B55F21000620005 and CNR Short Term Mobility Program.

Supporting Information Available

The Supporting information is available free of charge at .

- Details of force-field development of $CsPbI_3$, the computational domain setup, equilibrium molecular dynamics approach, vibrational density of states calculations, minimum thermal conductivity model.

References

(1) Dou, L.; Wong, A. B.; Yu, Y.; Lai, M.; Kornienko, N.; Eaton, S. W.; Fu, A.; Bischak, C. G.; Ma, J.; Ding, T.; Ginsberg, N. S.; Wang, L.-W.; Alivisatos, A. P.; Yang, P. Atomically thin two-dimensional organic-inorganic hybrid perovskites. *Science* **2015**, *349*, 1518–1521.

(2) Saliba, M.; Matsui, T.; Seo, J.-Y.; Domanski, K.; Correa-Baena, J.-P.; Nazeeruddin, M. K.; Zakeeruddin, S. M.; Tress, W.; Abate, A.; Hagfeldt, A.; Grätzel, M. Cesium-containing triple cation perovskite solar cells: improved stability, reproducibility and high efficiency. *Energy Environ. Sci.* **2016**, *9*, 1989–1997.

(3) Burschka, J.; Pellet, N.; Moon, S.-J.; Humphry-Baker, R.; Gao, P.; Nazeeruddin, M. K.; Grätzel, M. Sequential deposition as a route to high-performance perovskite-sensitized solar cells. *Nature* **2013**, *499*, 316.

(4) Zhu, H.; Fu, Y.; Meng, F.; Wu, X.; Gong, Z.; Ding, Q.; Gustafsson, M. V.; Trinh, M. T.; Jin, S.; Zhu, X.-Y. Lead halide perovskite nanowire lasers with low lasing thresholds and high quality factors. *Nature Materials* **2015**, *14*, 636.

(5) Snaith, H. J. Perovskites: The Emergence of a New Era for Low-Cost, High-Efficiency Solar Cells. *The Journal of Physical Chemistry Letters* **2013**, *4*, 3623–3630.

(6) Fang, Y.; Dong, Q.; Shao, Y.; Yuan, Y.; Huang, J. Highly narrowband perovskite single-crystal photodetectors enabled by surface-charge recombination. *Nature Photonics* **2015**, *9*, 679.

(7) Yuan, M.; Quan, L. N.; Comin, R.; Walters, G.; Sabatini, R.; Voznyy, O.; Hoogland, S.; Zhao, Y.; Beauregard, E. M.; Kanjanaboos, P.; Lu, Z.; Kim, D. H.; Sargent, E. H. Perovskite energy funnels for efficient light-emitting diodes. *Nature Nanotechnology* **2016**, *11*, 872.

(8) Saparov, B.; Mitzi, D. B. Organic–Inorganic Perovskites: Structural Versatility for Functional Materials Design. *Chemical Reviews* **2016**, *116*, 4558–4596.

(9) Grancini, G.; Nazeeruddin, M. K. Dimensional tailoring of hybrid perovskites for photovoltaics. *Nature Reviews Materials* **2019**, *4*, 4–22.

(10) Huang, J.; Yuan, Y.; Shao, Y.; Yan, Y. Understanding the physical properties of hybrid perovskites for photovoltaic applications. *Nature Reviews Materials* **2017**, *2*, 17042.

(11) Li, Z.; Klein, T. R.; Kim, D. H.; Yang, M.; Berry, J. J.; van Hest, M. F. A. M.; Zhu, K. Scalable fabrication of perovskite solar cells. *Nature Reviews Materials* **2018**, *3*, 18017.

(12) Elbaz, G. A.; Ong, W.-L.; Doud, E. A.; Kim, P.; Paley, D. W.; Roy, X.; Malen, J. A. Phonon

Speed, Not Scattering, Differentiates Thermal Transport in Lead Halide Perovskites. *Nano Letters* **2017**, *17*, 5734–5739, PMID: 28806090.

(13) Qian, X.; Gu, X.; Yang, R. Lattice thermal conductivity of organic-inorganic hybrid perovskite CH3NH3PbI3. *Applied Physics Letters* **2016**, *108*, 063902.

(14) Wang, M.; Lin, S. Anisotropic and Ultralow Phonon Thermal Transport in Organic-Inorganic Hybrid Perovskites: Atomistic Insights into Solar Cell Thermal Management and Thermoelectric Energy Conversion Efficiency. *Advanced Functional Materials* **2016**, *26*, 5297–5306.

(15) Ma, H.; Li, C.; Ma, Y.; Wang, H.; Rouse, Z. W.; Zhang, Z.; Slebodnick, C.; Alatas, A.; Baker, S. P.; Urban, J. J.; Tian, Z. Supercompliant and Soft $(CH_3NH_3)_3Bi_2I_9$ Crystal with Ultralow Thermal Conductivity. *Phys. Rev. Lett.* **2019**, *123*, 155901.

(16) Dualeh, A.; Gao, P.; Seok, S. I.; Nazeeruddin, M. K.; Grätzel, M. Thermal Behavior of Methylammonium Lead-Trihalide Perovskite Photovoltaic Light Harvesters. *Chemistry of Materials* **2014**, *26*, 6160–6164.

(17) Filippetti, A.; Caddeo, C.; Delugas, P.; Mattoni, A. Appealing Perspectives of Hybrid Lead–Iodide Perovskites as Thermoelectric Materials. *J. Phys. Chem. C* **2016**, *120*, 28472–28479.

(18) Peierls, R. Zur kinetischen Theorie der Wärmeleitung in Kristallen. *Annalen der Physik* **1929**, *395*, 1055–1101.

(19) Srivastava, G. Phonon conductivity of insulators and semiconductors. *J. Phys. Chem. Solids* **1980**, *41*, 357 – 368.

(20) Dove, M. T. *Introduction to Lattice Dynamics*; Cambridge University Press: Cambridge, 1993; pp 240–253.

(21) Ziman, J. M. *Electrons and Phonons*; Clarendon Press: Oxford, 1960.

(22) Kittel, C. *Introduction to Solid State Physics*, 6th ed.; John Wiley & Sons, Inc.: New York, 1986.

(23) Klemens, P. G. The scattering of low-frequency lattice waves by static imperfections. *Proceedings of the Physical Society. Section A* **1955**, *68*, 1113–1128.

(24) Allen, P. B.; Feldman, J. L. Thermal Conductivity of Glasses: Theory and Application to Amorphous Si. *Phys. Rev. Lett.* **1989**, *62*, 645–648.

(25) Allen, P. B.; Feldman, J. L. Thermal conductivity of disordered harmonic solids. *Phys. Rev. B* **1993**, *48*, 12581–12588.

(26) Zhu, T.; Ertekin, E. Mixed phononic and non-phononic transport in hybrid lead halide perovskites: glass-crystal duality, dynamical disorder, and anharmonicity. *Energy Environ. Sci.* **2019**, –.

(27) Simoncelli, M.; Marzari, N.; Mauri, F. Unified theory of thermal transport in crystals and glasses. *Nature Physics* **2019**, *15*, 809–813.

(28) Allen, P. B.; Feldman, J. L.; Fabian, J.; Wooten, F. Diffusons, locons and propagons: Character of atomie yibrations in amorphous Si. *Philosophical Magazine Part B* **1999**, *79*, 1715–1731.

(29) Seyf, H. R.; Yates, L.; Bougher, T. L.; Graham, S.; Cola, B. A.; Detchprohm, T.; Ji, M.-H.; Kim, J.; Dupuis, R.; Lv, W.; Henry, A. Rethinking phonons: The issue of disorder. *npj Computational Materials* **2017**, *3*, 49.

(30) Mattoni, A.; Filippetti, A.; Saba, M. I.; Caddeo, C.; Delugas, P. Temperature Evolution of Methylammonium Trihalide Vibrations at the Atomic Scale. *The Journal of Physical Chemistry Letters* **2016**, *7*, 529–535.

(31) Lee, W.; Li, H.; Wong, A. B.; Zhang, D.; Lai, M.; Yu, Y.; Kong, Q.; Lin, E.; Urban, J. J.;

Grossman, J. C.; Yang, P. Ultralow thermal conductivity in all-inorganic halide perovskites. *Proceedings of the National Academy of Sciences* **2017**,

(32) Mattoni, A.; Filippetti, A.; Saba, M. I.; Delugas, P. Methylammonium Rotational Dynamics in Lead Halide Perovskite by Classical Molecular Dynamics: The Role of Temperature. *The Journal of Physical Chemistry C* **2015**, *119*, 17421–17428.

(33) Koza, M. M.; Johnson, M. R.; Viennois, R.; Mutka, H.; Girard, L.; Ravot, D. Breakdown of phonon glass paradigm in La- and Ce-filled Fe4Sb12 skutterudites. *Nature Materials* **2008**, *7*, 805–810.

(34) Yue, S.-Y.; Zhang, X.; Qin, G.; Yang, J.; Hu, M. Insight into the collective vibrational modes driving ultralow thermal conductivity of perovskite solar cells. *Phys. Rev. B* **2016**, *94*, 115427.

(35) Li, B.; Kawakita, Y.; Liu, Y.; Wang, M.; Matsuura, M.; Shibata, K.; Ohira-Kawamura, S.; Yamada, T.; Lin, S.; Nakajima, K.; Liu, S. F. Polar rotor scattering as atomic-level origin of low mobility and thermal conductivity of perovskite CH3NH3PbI3. *Nature Communications* **2017**, *8*, 16086 EP –.

(36) Pisoni, A.; Jacimovic, J.; Barisic, O. S.; Spina, M.; Gaal, R.; Forro, L.; Horvath, E. Ultra-Low Thermal Conductivity in Organic-Inorganic Hybrid Perovskite CH3NH3PbI3. *The Journal of Physical Chemistry Letters* **2014**, *5*, 2488–2492, PMID: 26277821.

(37) Giri, A.; Chen, A. Z.; Mattoni, A.; Aryana, K.; Zhang, D.; Hu, X.; Lee, S.-H.; Choi, J. J.; Hopkins, P. E. Ultralow Thermal Conductivity of Two-Dimensional Metal Halide Perovskites. *Nano Letters* **2020**, *20*, 3331–3337.

(38) Hata, T.; Giorgi, G.; Yamashita, K. The Effects of the Organic-Inorganic Interactions on the Thermal Transport Properties of CH3NH3PbI3. *Nano Letters* **2016**, *16*, 2749–2753, PMID: 27003760.

(39) Caddeo, C.; Melis, C.; Saba, M. I.; Filippetti, A.; Colombo, L.; Mattoni, A. Tuning the thermal conductivity of methylammonium lead halide by the molecular substructure. *Phys. Chem. Chem. Phys.* **2016**, *18*, 24318–24324.

(40) Zhou, J.-J.; Bernardi, M. Predicting charge transport in the presence of polarons: The beyond-quasiparticle regime in $\mathrm{SrTiO_3}$. *Phys. Rev. Research* **2019**, *1*, 033138.

(41) Soo, Y. H.; Ng, S. A.; Wong, Y. H.; Ng, C. Y. Thermal stability enhancement of perovskite MAPbI3 film at high temperature (150 °C) by PMMA encapsulation. *J. Mater. Sci. Mater. Electron.* **2021**, *32*, 14885–14900.

(42) Mattoni, A.; Filippetti, A.; Caddeo, C. Modeling hybrid perovskites by molecular dynamics. *J. Phys. Condens. Matter* **2017**, *29*, 043001.

(43) Caddeo, C.; Filippetti, A.; Mattoni, A. The dominant role of surfaces in the hysteretic behavior of hybrid perovskites. *Nano Energy* **2020**, *67*, 104162.

(44) Mattoni, A.; Caddeo, C. Dielectric function of hybrid perovskites at finite temperature investigated by classical molecular dynamics. *J. Chem. Phys.* **2020**, *152*, 104705.

(45) Delugas, P.; Caddeo, C.; Filippetti, A.; Mattoni, A. Thermally Activated Point Defect Diffusion in Methylammonium Lead Trihalide: Anisotropic and Ultrahigh Mobility of Iodine. *J. Phys. Chem. Lett.* **2016**, *7*, 2356–2361.

(46) Cahill, D. G.; Watson, S. K.; Pohl, R. O. Lower limit to the thermal conductivity of disordered crystals. *Phys. Rev. B* **1992**, *46*, 6131–6140.

(47) Manley, M. E.; Hong, K.; Yin, P.; Chi, S.; Cai, Y.; Hua, C.; Daemen, L. L.; Hermann, R. P.; Wang, H.; May, A. F.; Asta, M.; Ahmadi, M. Giant isotope effect on phonon dispersion and thermal conductivity in methylammonium lead iodide. *Sci. Adv.* **2020**, *6*.

(48) Kovalsky, A.; Wang, L.; Marek, G. T.; Burda, C.; Dyck, J. S. Thermal Conductivity of

CH3NH3PbI3 and CsPbI3: Measuring the Effect of the Methylammonium Ion on Phonon Scattering. *The Journal of Physical Chemistry C* **2017**, *121*, 3228–3233.

(49) Christensen, M.; Abrahamsen, A. B.; Christensen, N. B.; Juranyi, F.; Andersen, N. H.; Lefmann, K.; Andreasson, J.; Bahl, C. R. H.; Iversen, B. B. Avoided crossing of rattler modes in thermoelectric materials. *Nature Materials* **2008**, *7*, 811–815.

(50) Vining, C. B. Half-full glasses. *Nature Materials* **2008**, *7*, 765–766.

Graphical TOC Entry